Synthetic Metals 209 (2015) 128–134

Contents lists available at ScienceDirect

Synthetic Metals

journal homepage: www.elsevier.com/locate/synmet

Temperature dependence of cesium carbonate-doped electron transporting layers on organic light-emitting diodes

Richard Fu*, Eric Forsythe, Jianmin Shi, Merric Srour, Steven Blomquist, David Morton

U.S Army Research Laboratory, 2800 Powder Mill Road, Adelphi, MD 20783-1138, USA

ARTICLE INFO

Article history:
Received 4 June 2015
Received in revised form 13 July 2015
Accepted 17 July 2015
Available online 29 July 2015

Keywords:
Organic materials
OLED devices
Electroluminescence
Electron transport
Electron injection
Cesium carbonate doping

ABSTRACT

The temperature dependence and electronic transport properties of 1, 3, 5-*tri*(1-phenyl-1H-benzo[d] imidazol-2-yl) phenyl (TPBI) and 8-hydroxyquinoline aluminum (Alq) electron transporting layers (ETL) have been investigated as a function of cesium carbonate (Cs_2CO_3) doping for organic light emitting devices. The current-voltage and light emission characteristics were measured as a function of the Cs_2CO_3 doped ETL thickness at both room temperature and cryogenic (10–300 K). The current density (J) for the Alq:Cs_2CO_3 ETL device increased for an ETL thickness between 100 and 300 Å, with no further increase in the ETL beyond 300 Å, indicating an electron injection limited contact. Conversely, the J for the TPBI:Cs_2CO_3 ETL device did not saturate for increasing ETL thicknesses confirming the TPBI:Cs_2CO_3 devices have a near-ohmic cathode contact. The correlation of current density–voltage (*J–V*) and luminance-voltage (*L–V*) for both Alq:Cs_2CO_3 and TPBI:Cs_2CO_3 devices were studied over temperatures from 10 to 300 K. Both increased with increasing temperature; however, Cs_2CO_3-doped TPBI devices were more effective than Cs_2CO_3-doped Alq devices. The observed differences between Alq and TPBI may be attributed to the exposed nitrogen electron pair in the electronic structure.

Published by Elsevier B.V.

1. Introduction

Research in organic light-emitting diode (OLED) displays has been attaining greater momentum during the last decade due to their capacity to form flexible displays [1]. OLEDs have many advantages including easy processing, robustness and inexpensive foundry compared to inorganic counterparts, and they have emerged as the second most important display technology for commercial applications [2]. OLED-based displays are integrated in many of today's portable phones due to the visual quality, low profile, and low power consumption. These same attributes have led to recent announcements of OLED television technology as well as OLED-based displays integrated on plastic substrates enabling a new generation of information technologies [3]. In particular, the low power consumption of OLED-displays has attracted strong interest for many portable commercial and military applications [4]. In fact, the OLED display is rapidly moving from fundamental research into industrial product, creating many new challenges like lower operation voltage and power consumption, and operating under extreme environmental conditions [5,6]. Research to lower the OLED operating voltage has led to the development of enhanced electron injection with the integration of alkali metals and alkali metal complexes (such as cesium carbonate, Cs_2CO_3) as a sub-monolayer deposited between the organic electron transporting layer (ETL) and the metal cathode [7,8]. Similarly, the enhancement of the electron transport properties of the bulk organic ETL has been demonstrated by co-evaporating alkali metals and complexes with the organic ETL material [9–12].

Furthermore, the users need high performance displays that can withstand the different environmental conditions, which are used in a wide range of sights and vision systems that can be deployed in very different locations with extreme environmental conditions, such as the mountains in winter or the desert in summer. How the device responds to different temperature ambience has also attracted the attention of scientists [13]. A few researchers have been investigated the temperature dependence of 8-hydroxyquinolinato aluminum (Alq) ETLs on OLEDs [14,15]. However, the cryogenic temperature effects of 1, 3, 5-*tri*(1-phenyl-1H-benzo[d]imidazol-2-yl) phenyl (TPBI) ETLs on OLEDs has not yet been explored.

In this paper, we discuss the electron injection and electron transport characteristics of simple bi-layer OLEDs with 2 different ETLs: Alq and TPBI. TPBI has demonstrated blue fluorescent emission and electron transport properties for OLED-based displays [16,17], while Alq is a green OLED. The results in this paper demonstrate different electron transport and injection

* Corresponding author. Fax: +1 301 394 0310.
E-mail address: richard.x.fu.civ@mail.mil (R. Fu).

http://dx.doi.org/10.1016/j.synthmet.2015.07.025
0379-6779/Published by Elsevier B.V.

characteristics between ETLs consisting of TPBI and Alq doped with Cs_2CO_3 at a fixed concentration of 7% by weight. We use Cs_2CO_3-doped Alq and TPBI as the ETL materials to decrease the operating voltage and power consumption, and systematically investigate cryogenic temperature dependence of Cs_2CO_3-doped Alq and TPBI on an OLED. The mechanisms of the charge-transfer (CT) complex in Cs_2CO_3-doped TPBI are discussed, which provides insight into designing future materials and device structure with enhanced performance.

2. Experiment

The ETL organic materials used were Alq, and TPBI, as illustrated in the Fig. 1 along with the energy level diagram for the simple bi-layer devices architecture. In Fig. 1, the energy level alignment for TPBI shows a Highest Occupied Molecular Orbital (HOMO) state at 6.2 eV below the vacuum level as compared to HOMO of 5.8 eV for Alq [16–18]. The 2 ETL organic materials have the same lowest occupied molecular orbital (LUMO) state relative to the vacuum level implying the electron injection barrier is similar for the undoped TPBI and Alq ETL materials.

The OLEDs were fabricated starting with a standard indium-tin-oxide (ITO) coated glass substrate preparations. Six device cells, with 4 identical devices per cell, were fabricated in a single deposition run for the 2 ETL experiments, TPBI and Alq, respectively. A common (750 Å) 4,4′-bis[N-(1-nathyl)-*N*-phenyl-amino]biphenyl (NPB) hole transporting layer was first deposited on the ITO substrates at 2.0×10^{-6} Torr followed by the EML and ETL layers at a total constant thickness of 600 Å, and a common magnesium (Mg)-silver (Ag) (10 parts Mg to 1 part Ag) cathode. For both sets of devices, the EML was the undoped ETL organic material, TPBI and Alq respectively. The 6 device cells for the TPBI and Alq experimental sets were fabricated as follows:

A. ITO/NPB (750 Å)/EML (600 Å)/ETL (0 Å)/Mg:Ag;
B. ITO/NPB (750 Å)/EML (500 Å)/ETL (100 Å)/Mg:Ag;
C. ITO/NPB (750 Å)/EML (300 Å)/ETL (300 Å)/Mg:Ag;
D. ITO/NPB (750 Å) /EML (100 Å)/ETL (500 Å)/Mg:Ag;
E. ITO/NPB (750 Å)/EML (50 Å)/ETL (550 Å)/Mg:Ag;
F. ITO/NPB (750 Å) /EML (0 Å)/ETL (600 Å)/Mg:Ag.

The doped ETL for the 2 experiments was the co-deposition of TPBI or Alq and Cs_2CO_3 at 7% relative molecular weights. The device cells were sealed and the current density as a function of current density-voltage (*J*–*V*) measurements were conducted with a Keithley 2400 source meter and the light emission properties were measured with a Photoresearch 650 spectrophotometer with the Keithley.

Fig. 2 shows the cryogenic temperature test set-up. The OLED is mounted on a copper (Cu) plate in a cryogenic chamber which acts as a sample holder and is capable of being cooled down to 10 K by a helium pump. The silicon (Si) photodetector is mounted inside the chamber about 2–3 mm from the device surface (not in contact with the sample mounting plate) with feedthroughs that connect it to electronics outside of the chamber. The cryogenic chamber was kept at the vacuum of 10^{-6} Torr during the experiment.

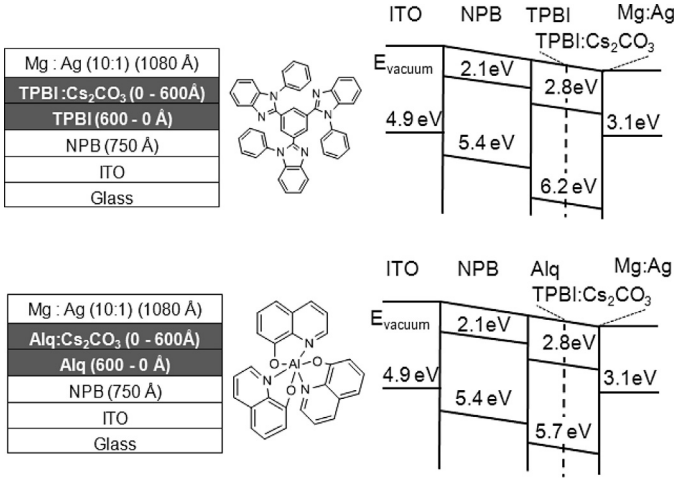

Fig. 1. The TPBI and Alq device configuration with gray regions indicating the thickness ratio of a doped ETL and an undoped emitting layer (EML), where the total ETL+EML layer thickness is constant at 600 Å for all devices investigated. The corresponding energy level diagrams (not including the interface energy level bending) are shown with the TPBI and Alq molecular structures.

3. Results and discussion

3.1. Room temperature characteristics of Cs_2CO_3-doped Alq and TPBI

Fig. 3 shows the current density (*J*) as a function of operating voltage (*V*) (*J*–*V*). Fig. 3a, the Alq:Cs_2CO_3 ETL OLEDs, shows an initial rapid increase in *J* at ETL 100 Å, then slowly increasing until the Alq:Cs_2CO_3 ETL layer is 600 Å (EML = 0 Å). This data point suggests the hole injection into the Alq:Cs_2CO_3 ETL is reduced. By comparison, the TPBI:Cs_2CO_3 *J* continuously increases to the ETL thickness of 600 Å in Fig. 3b.

Fig. 4 is a summary plot of the current density (*J*) at 4 V for the 6 device cells as a function of Alq:Cs_2CO_3 and TPBI:Cs_2CO_3 ETL thickness. *J* at 4 V level off after the Alq ETL doped layer thickness 300 Å. From the inset in Fig. 4, the total contact resistance is represented by R_1, R_{ETL} and represents the resistance of the Alq:Cs_2CO_3 ETL, and R_{EML} is the undoped emission layer Alq EML. As the Alq ETL thickness increases, total resistance, $R_{EML} + R_{ETL}$, will decrease. Thus, the saturation in the current density beyond 300 Å for the Alq:Cs_2CO_3 ETL thickness indicates the contact resistance R_1 dominates the bi-layer electron transport properties as the contact cannot supply additional current as the bulk resistance decreases [18]. Thus, the Alq:Cs_2CO_3 devices are contact limited. Conversely, the TPBI:Cs_2CO_3 devices demonstrate a constant increase in *J* at 4 V as the TPBI:Cs_2CO_3 thickness increases relative to the undoped emission layer TPBI EML. Again, the electron resistance, R_{EML}+R_{ETL} is decreasing and the total device current density, *J*, is increasing, indicating the devices with TPBI:Cs_2CO_3 ETLs are bulk limited, or the contact is near ohmic for all devices. The molecular structures of the TPBI and Alq molecules illustrated in Fig. 1 suggest an explanation for the electron transport differences. The TPBI molecule has 6 N atoms as compared to 3 N atoms in Alq. The addition exposed N electron pairs in TPBI may contribute to improve bulk electron transport properties in Cs_2CO_3-doped devices.

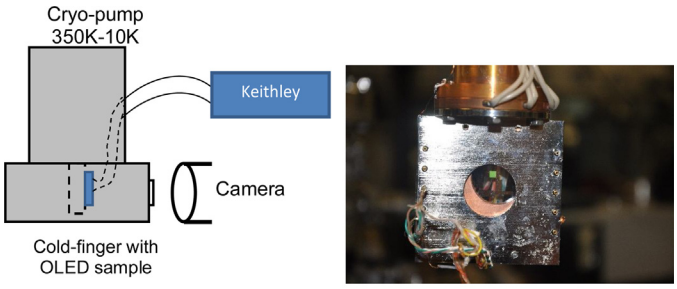

Fig. 2. (a) Schematic of the cryogenic temperature test setup and (b) a close-up of the OLED sample on the cold-finger.